JOC Article

A DFT Study of the Mechanisms and Regio- and Stereochemistry of the Lewis Acid-Catalyzed Reactions of 5-Alkoxyoxazoles with Aldehydes: Aryl Substitution at the 2-Position of 5-Alkoxyoxazole Is Critical to the Formation of 4-Alkoxycarbonyl-2-oxazoline

Zhi-Xiang Yu*,† and Yun-Dong Wu*

Department of Chemistry, The Hong Kong University of Science & Technology, Clearwater Bay, Kowloon, Hong Kong, China

zhixiang@chem.ucla.edu; chydwu@ust.hk

Received August 16, 2002

Density functional theory at the B3LYP/6-31G* level has been used to study the mechanisms and regio- and stereochemistry of the Lewis acid-catalyzed reactions of aldehydes with 5-alkoxyoxazoles. Similar to the uncatalyzed reaction between aldehyde and 5-methoxyoxazole, which has an activation energy of 30.5 kcal/mol and intrinsically favors production of 2-alkoxycarbonyl-3-oxazoline, the Lewis acid-catalyzed reaction also prefers to generate 2-alkoxycarbonyl-3-oxazoline in a more efficient way with an activation energy of about 3 kcal/mol (with respect to separated acetaldehyde−$AlCl_3$ complex and 5-methoxyoxazole) in the gas phase. Only when an aryl group is introduced to the 2 position of 5-alkoxyoxazoles can the Lewis acid-catalyzed reactions furnish 4-alkoxycarbonyl-2-oxazolines. The reasons for this switch of regiochemistry and the factors affecting the stereochemistry are discussed.

1. Introduction

In the previous paper,[1] we presented a study on the reaction mechanisms of 5-alkoxyoxazole with thioacetaldehyde, nitrosomethane, and acetaldehyde, indicating that these three reactions intrinsically favor similar mechanisms (via initial Diels−Alder (DA) reaction followed by concerted ring-opening−ring-closing (RORC) or stepwise ring-opening (RO) and ring-closing (RC) reactions) to generate 3-thiazoline, 1,2,4-oxadiazoline, and 3-oxazoline, respectively.[1,2] It is predicted that reaction between 5-alkoxyoxazole and acetaldehyde could not be carried out under thermal reaction conditions due to the 30.5 kcal/mol activation energy required (this does not include the entropy loss), due to the endothermicity of the DA reaction step and the energy-demanding RORC step. This is the reason all the reported reactions between aldehydes and 5-alkoxyoxazoles were conducted in the presence of Lewis acid (LA) catalysts.[3,4] It is understandable that LAs are used in order to reduce the activation barrier. However, an interesting and important question we want to address here is why all of the reported LA-catalyzed reactions gave rise to 2-oxazolines instead of 3-oxazolines (Scheme 1).[3,4] Notably, 2-oxazolines are more versatile building blocks in organic synthesis as masked β-hydroxy amino acids and 2-amino-1,3-diols.[5−8]

SCHEME 1

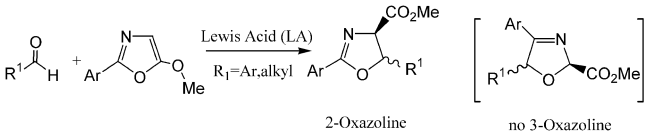

Meanwhile, we are very interested in the stereochemistry of the LA-catalyzed reactions; when the catalysts

† Present address: Department of Chemistry and Biochemistry, University of California, Los Angeles, CA 90095-1569. Fax: (310) 206-1843.

(1) Yu, Z.-X.; Wu, Y-.D. *J. Org. Chem.* **2002**, *67*, 412.

(2) Unless otherwise mentioned, 3- and 2-oxazolines in this paper referred to 2-alkoxycarbonyl-3-oxazoline and 4-alkoxycarbonyl-2-oxazoline, respectively.

(3) Suga, H.; Shi, X.; Fujieda, H.; Ibata, T. *Tetrahedron Lett.* **1991**, *32*, 6911. (b) Suga, H.; Shi, X.; Ibata, T. *J. Org. Chem.* **1993**, *58*, 7397. (c) Suga, H.; Ibata, T. *Tetrahedron Lett.* **1989**, *39*, 869. (d) Suga, H.; Ikai, K.; Ibata, T. *J. Org. Chem.* **1999**, *64*, 7040. (e) Suga, H.; Shi, X.; Ibata, T. *Bull. Chem. Soc. Jpn.* **1998**, *71*, 1231. (f) Suga, H.; Shi, X.; Ibata, T.; Kakehi, A. *Heterocycles* **2001**, *55*, 1711. (g) Suga, H.; Fujieda, H.; Hirotsu, Y.; Ibata, T. *J. Org. Chem.* **1994**, *59*, 3359. (h) For a recent review of these Lewis acid-catalyzed reactions, see: (i) Suga, H.; Ibata, T. *Rev. Heteroat. Chem.* **1999**, *21*, 195.

(4) Evans, D. A.; Janey, J. M.; Magomedov, N.; Tedrow, J. *Angew. Chem., Int. Ed.* **2001**, *40*, 1884.

(5) For a review of the syntheses of 4-alkoxycarbonyl-2-oxazoline using isocyanoacetates and conversion to β-hydroxyamine acids, see: Matsumoto, K.; Moriya, T.; Suzuki, M. J. *Synth. Org. Chem. Jpn.* **1988**, *43*, 7664.

(6) (a) Hoppe, D.; Schöllkopphf, U. *Justus Liebigs Ann. Chem.* **1972**, *763*, 1. (b) Matsumoto, K.; Urabe, Y.; Ozaki, Y.; Iwasaki, T.; Miyoshi, M. *Agric. Biol. Chem.* **1975**, *39*, 1869. (c) Matsumoto, K.; Ozaki, Y.; Suzuki, M.; Miyoshi, M. *Agric. Biol. Chem.* **1976**, *40*, 2045. (d) Ozaki, Y.; Matsumoto, K.; Miyoshi, M. *Agric. Biol. Chem.* **1978**, *42*, 1565.

(7) (a) Ito, Y.; Sawamura, M.; Hayashi, T. *J. Am. Chem. Soc.* **1986**, *108*, 6405. (b) Ito, Y.; Sawamura, M.; Hayashi, T. *Tetrahedron Lett.* **1987**, *28*, 6215; **1988**, *29*, 239. (c) Ito, Y.; Sawamura, M.; Shirakawa, E.; Hayashizaki, K.; Hayashi, T. *Tetrahedron Lett.* **1988**, *29*, 235. (d) Ito, Y.; Sawamura, M.; Shirakawa, E.; Hayashizaki, K.; Hayashi, T. *Tetrahedron* **1988**, *44*, 5253.

(8) The stereoselective synthesis of α-amino-β-hydroxy acids is an intensive research field, since these acids are building blocks of numerous peptide-based natural products, including the vancomycin antibiotics; see references in ref 4.

10.1021/jo0263317 CCC: $25.00
Published on Web 12/17/2002

SCHEME 2

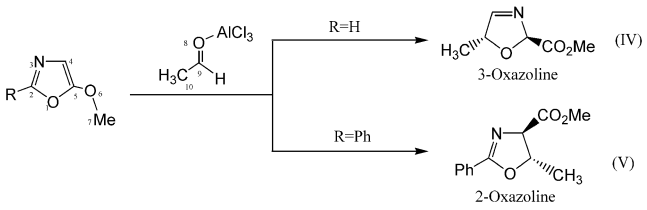

are $SnCl_4$, $TiCl_4$, or $AlCl_2Me$, the dominant product is often *trans*-3-oxazoline, even though the ratio of trans/cis varies when different catalysts and solvents are used. However, when bulky catalysts such as BINOL−AlMe and Salen−aluminum complexes are used, the final major product is *cis*-2-oxazoline. Enantioselectivity has also been achieved by Suga and Ibata using chiral BINOL−AlMe[3] and by Evans using Salen−aluminum complexes.[4] The reason for the cis or trans selectivity is not clear. Therefore, a theoretical rationale for the reaction mechanism is indispensable. In this paper, we will only discuss the stereoselectivity when $SnCl_4$, $TiCl_4$, and $AlCl_2Me$ are used as the LA catalysts. The LA catalyst for our theoretical modeling is $AlCl_3$. The amazingly high cis selectivity and enantioselectivy achieved by Evans' chiral Salen−aluminum catalysts is the target of an ongoing investigation and will be reported in due course.

Two LA-catalyzed model reactions, referred to here as reactions IV and V (reactions I−III were discussed in the previous paper[1]) and shown in Scheme 2, have been modeled to address the above-mentioned issues of reaction mechanism and regio- and stereochemistry. Our studies indicated that the generation of 2- or 3-oxazoline is the consequence of the two competitive mechanisms shown in Scheme 3. The first step is the aldol-like or nucleophilic addition (NA) of 5-alkoxyoxazole to aldehyde, which can occur either at the C_2 (manifold A) or C_4 (manifold C) position. The zwitterionic intermediate then undergoes fragmentation and cyclization via either stepwise RO and RC reactions or concerted RORC reaction to give the products. We will demonstrate that the LA catalyst significantly accelerates the reaction between aldehyde and 5-alkoxyoxazole, which intrinsically favors production of 3-oxazoline. Only when an aryl group is present in the C_2-position will the generation of 2-oxazoline be favored.

2. Computational Methodology

All the calculations were performed with the Gaussian 98 program.[9] Geometries were fully optimized with the density functional method B3LYP[10,11] using the standard 6-31G* basis set.[12] Harmonic vibration frequency calculations were carried out for all the stationary points of reaction IV and several key transition states of reaction V (**67c**, **73a**, **69**, and **75**) to confirm each structure being either a minimum (no imaginary frequency) or a transition state (one imaginary frequency). Intrinsic reaction coordinate (IRC)[13] calculations were traced in some doubtful cases to ensure that the transition states did in fact connect the proper minima. Solvent effect has been considered by using the PCM[14] model in CH_2Cl_2 ($\epsilon = 8.93$) based on the gas-phase structures computed with the DFT method. Unless otherwise mentioned, the atom numbering used is referred to that shown in Scheme 2 and the relative energies are zero-point energy (ZPE) corrected (ΔE_0). In addition, the discussion of the stereochemistry of reactions IV and V is based on the assumption that the distribution of final cis and trans product is kinetically controlled. Actually, in the presence of strong Lewis acids, such as $SnCl_4$ or $TiCl_4$, *cis*-2-oxazolines could isomerize to thermodynamically more stable *trans*-2-oxazolines.[3,4]

SCHEME 3

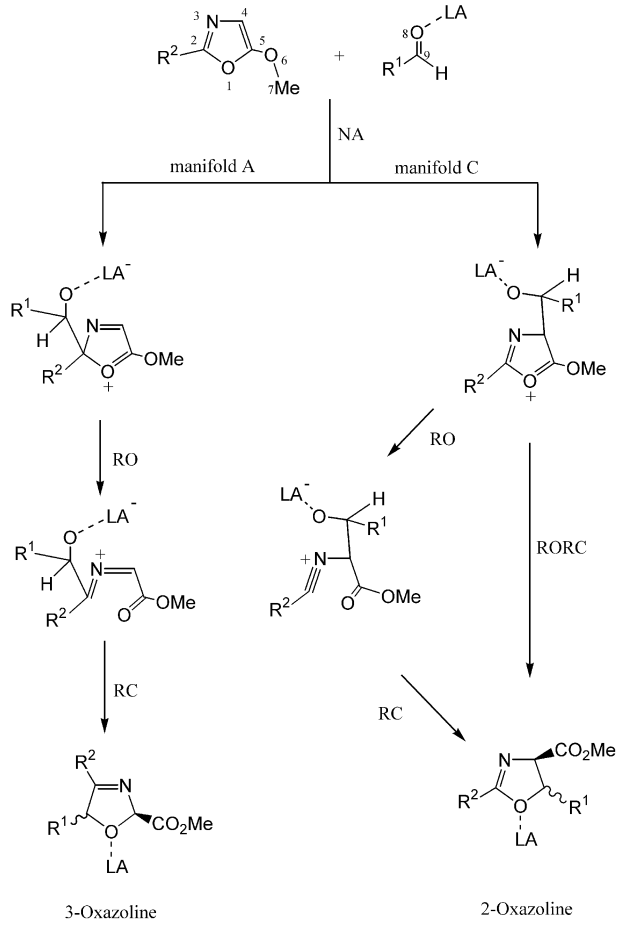

3. Results and Discussion

3.1. Competitive Complexation of $AlCl_3$ between $CH_3CH{=}O$ and Alkoxyoxazole. The coordination of the

(9) Frisch, M. J.; Trucks, G. W.; Schlegel, H. B.; Scuseria, G. E.; Robb, M. A.; Cheeseman, J. R.; Zakrzewski, V. G.; Montgomery, J. A.; Stratmann, R. E.; Burant, J. C.; Dapprich, S.; Millam, J. M.; Daniels, A. D.; Kudin, K. N.; Strain, M. C.; Farkas, O.; Tomasi, J.; Barone, V.; Cossi, M.; Cammi, R.; Mennucci, B.; Pomelli, C.; Adamo, C.; Clifford, S.; Ochterski, J.; Petersson, G. A.; Ayala, P. Y.; Cui, Q.; Morokuma, K.; Malick, D. K.; Rabuck, A. D.; Raghavachari, K.; Foresman, J. B.; Cioslowski, J.; Oritz, J. V.; Stefanov, B. B.; Liu, G.; Liashenko, A.; Piskorz, P.; Komaromi, I.; Gomperts, R.; Martin, R. L.; Fox, D. J.; Keith, T.; Al-Laham, M. A.; Peng, C. Y.; Nanayakkara, A.; Gonzalez, C.; Challacombe, M.; Gill, P. M. W.; Johnson, B. G.; Chen, W.; Wong, M. W.; Andres, J. L.; Head-Gordon, M.; Replogle, E. S.; Pople, J. A. *Gaussian 98, Revision A.1;* Gaussian, Inc.: Pittsburgh, PA, 1998.

(10) (a) Becke, A. D. *J. Chem. Phys.* **1993**, *98*, 5648. (b) Lee, C.; Yang, W.; Parr, R. *Phys. Rev. B* **1988**, *37*, 785.

(11) For reviews of density-functional methods, see: (a) Parr, R. G.; Yang, W. *Density Functional Theory of Atoms and Molecules*; Oxford University Press: New York, 1989. (b) Ziegler, T. *Chem. Rev.* **1991**, *91*, 651. (c) *Density Functional Methods in Chemistry;* Labanowski, J., Andzelm, J., Eds.; Springer: Berlin, 1991.

(12) Hehre, W. J.; Radom, L.; Schleyer, P. v. R.; Pople, J. A. *Ab Initio Molecular Orbital Theory*; Wiley: New York, 1986.

(13) (a) Gonzalez, C.; Schlegel, H. B. *J. Chem. Phys.* **1989**, *90*, 2154. (b) Gonzalez, C.; Schlegel, H. B. *J. Chem. Phys.* **1990**, *94*, 2435.

(14) Tomasi, J.; Persico, M. *Chem. Rev.* **1994**, *94*, 2027.

SCHEME 4[a]

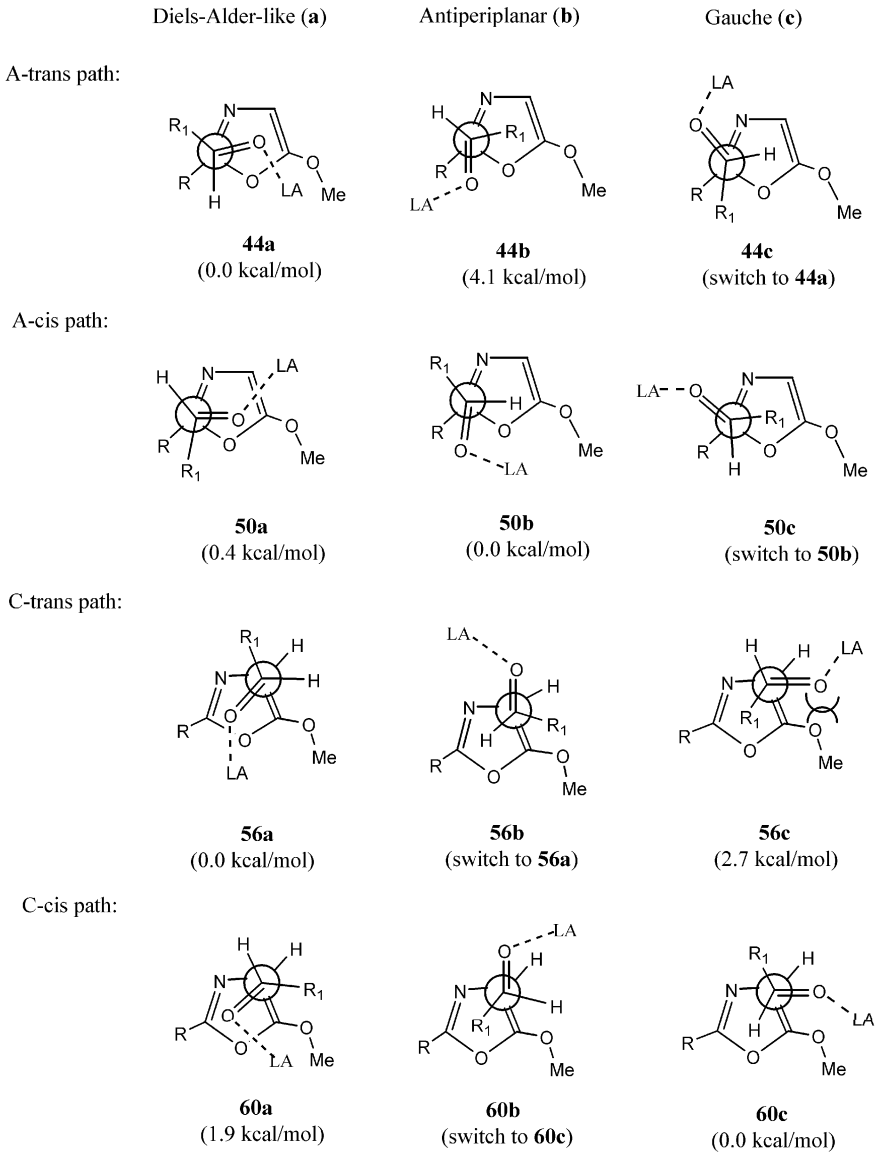

[a] The relative energies (without ZPE corrections) of the NA transition states for reaction IV (R^1=Me, R=H).

LA to the aldehyde has been extensively investigated, indicating that the *trans*-η^1-complex is the most stable one.[15,16] Our calculations at the B3LYP/6-31G* level confirm this, showing that the cis conformer (where the Al atom is coplanar with the plane of the carbonyl) is less stable than the trans conformer by 2.3 kcal/mol. The binding energy for $AlCl_3$ with aldehyde is −31.1 kcal/mol.

Competitive complexations of LA to the O_1, O_6, and N_3 atoms of 5-methoxyoxazole (MOX) are also possible in the reaction system. The calculated binding energies in terms of ΔE_{ele} (without ZPE corrections) of $AlCl_3$ to these basic sites are −16.5, −20.7, and −38.4 kcal/mol, respectively. Even though the N_3 atom of MOX is more efficient

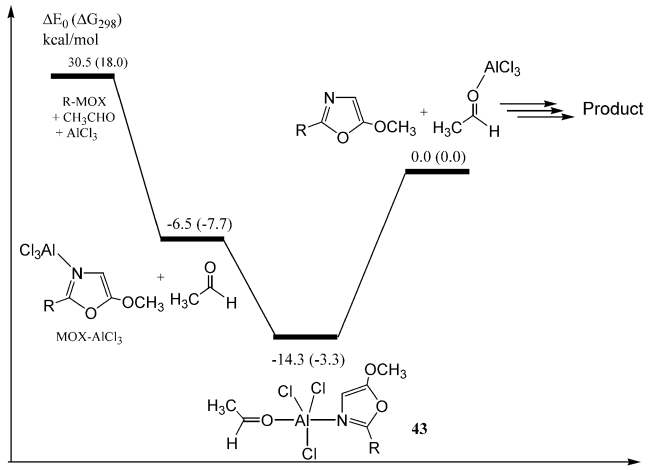

FIGURE 1. The complexation and $AlCl_3$-transfer processes. The B3LYP/6-31G* calculated relative energies are referred to those of the R=H system.

(15) Santelli, M.; Pons, J.-M. *Lewis Acids and Selectivity in Organic Synthesis*, CRC Press: Boca Raton, FL, 1996.

(16) (a) Reetz, M. T.; Hullman, M.; Massa, W.; Berger, S.; Rademacher, P.; Heymanns, P. *J. Am. Chem. Soc.* **1986**, *108*, 2405. (b) Nelson, D. J. *J. Org. Chem.* **1986**, *51*, 3185. (c) Gung, B. W.; Peat, A. J.; Snook, B. M.; Smith, D. T. *Tetrahedron Lett.* **1991**, *32*, 453. (d) Gung, B. W. *Tetrahedron Lett.* **1991**, *32*, 2867.

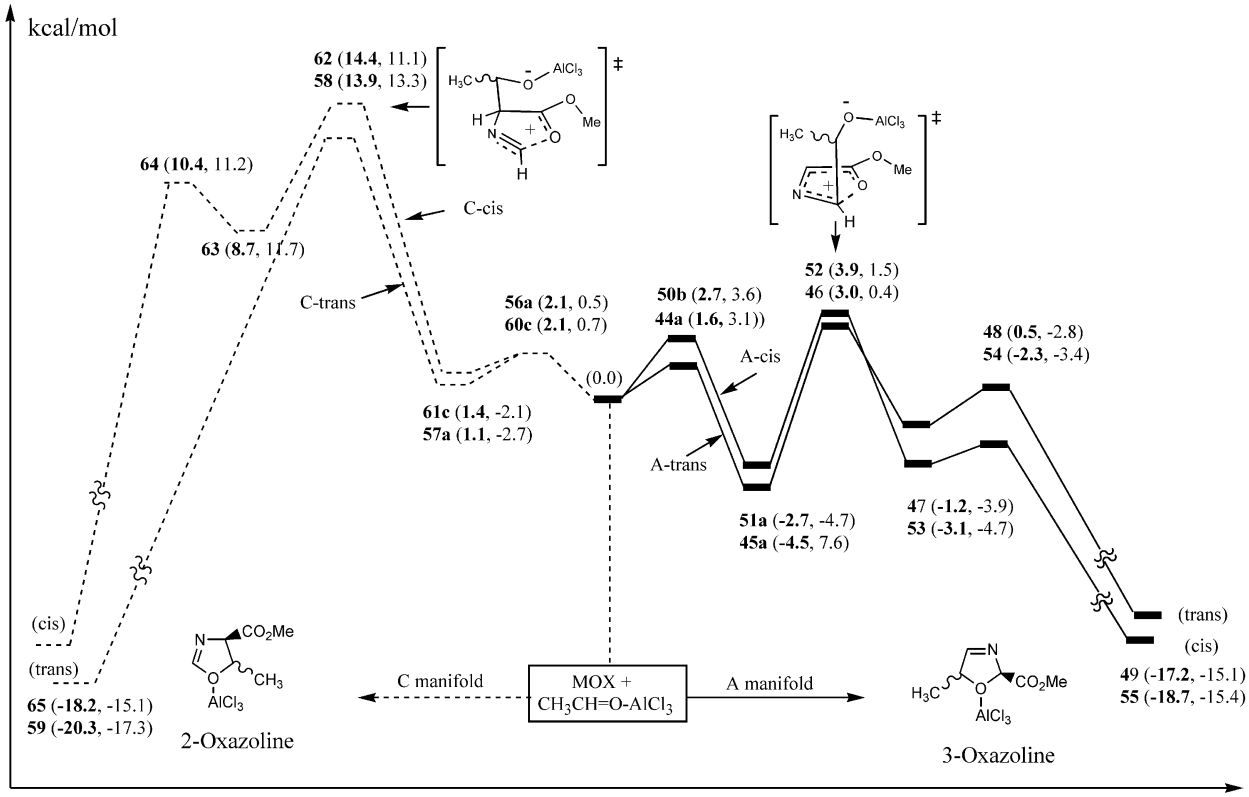

FIGURE 2. The potential energy surface of reaction IV computed at the B3LYP/6-31G* level. The solid and dashed lines represent the manifolds A and C, leading to 3- and 2-oxazolines, respectively. The bold and plain values in parentheses are the ZPE-corrected energies (E_0) in the gas phase and CH_2Cl_2, respectively.

SCHEME 5

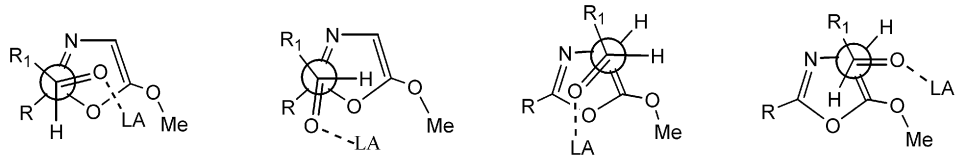

44a (1.6 kcal/mol) A-trans path

50b (2.7 kcal/mol) A-cis path

56a (2.1kcal/mol) C-trans path

60c (2.1 kcal/mol) C-cis path

SCHEME 6

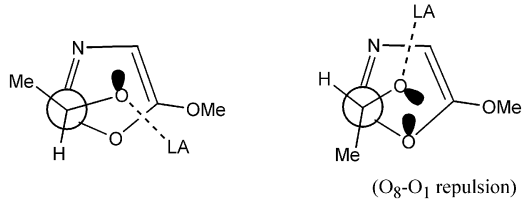

(O_8-O_1 repulsion)

SCHEME 7

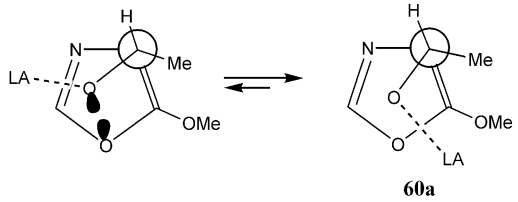

60a

for binding $AlCl_3$ than the oxygen atom of acetaldehyde by 6.5 kcal/mol in terms of ΔE_0, no Diels−Alder or nucleophilic addition transition states between acetaldehyde and MOX−$AlCl_3$ complex can be located (the reason for this dead-end reaction channel is possibly due to decrease of the HOMO energy (−10.43 eV) of MOX−$AlCl_3$ complex compared to that (−8.74 eV) of free MOX as well as a decrease of electron density in the five-membered ring). This suggests that there is a $AlCl_3$-transfer process to transfer $AlCl_3$ from MOX−$AlCl_3$ complex to CH_3CHO, and the resulting CH_3CHO−$AlCl_3$ complex can enter the reaction channel to complete the catalytic reaction (Figure 1). Our calculations estimated that about 6.5 kcal/mol is needed to transfer $AlCl_3$ from MOX−$AlCl_3$ to aldehyde (see Figure S1 in the Supporting Information for detailed discussion). As we will see later, the activation energies for reaction IV and V are around 3 kcal/mol with respect to the separated acetaldehyde−$AlCl_3$ complex and 5-methoxyoxazoles, meaning that the overall activation energies are 9.5 kcal/ mol with respect to MOX−$AlCl_3$ and aldehyde, if we consider this $AlCl_3$-transfer step. This overall activation energy of 9.5 kcal/

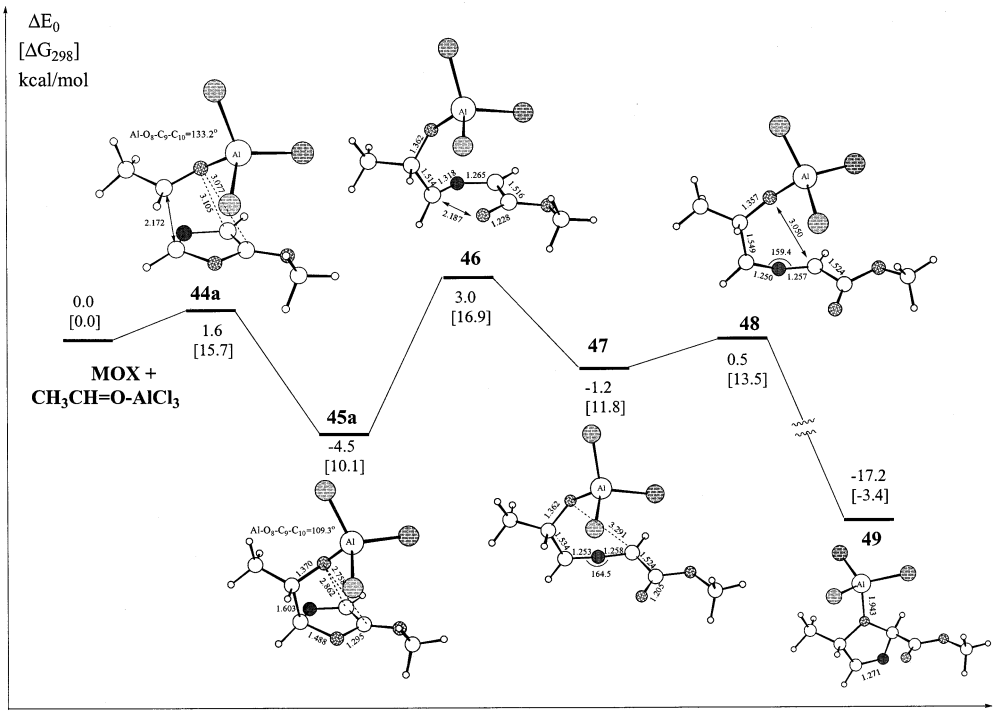

FIGURE 3. The potential energy surface of the A-trans path for reaction IV computed at the B3LYP/6-31G* level. The plain values are energies (kcal/mol) in terms of gas phase ΔE_0 and ΔG_{298} (in parentheses), respectively.

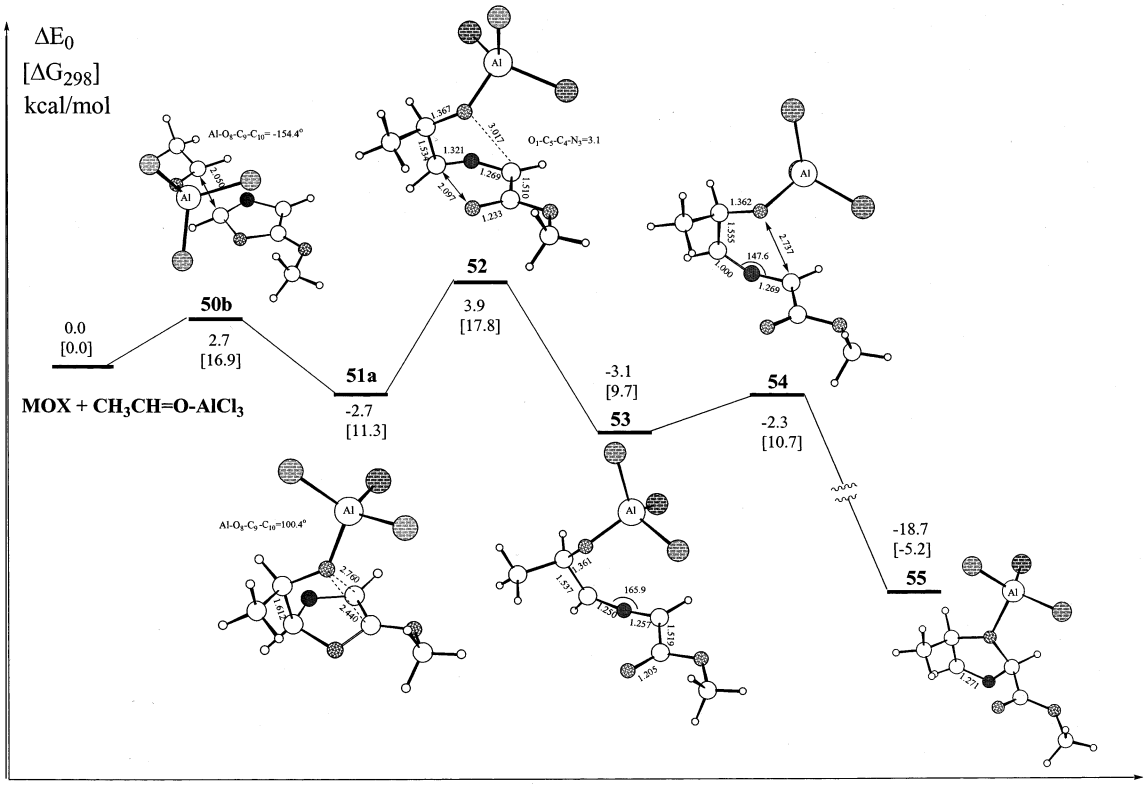

FIGURE 4. The potential energy surface of the A-cis path for reaction IV computed at the B3LYP/6-31G* level. The plain values are energies (kcal/mol) in terms of gas phase ΔE_0 and ΔG_{298} (in parentheses), respectively.

mol is still significantly less than that of the uncatalyzed reaction between 5-methoxyoxazole and aldehyde. Similar phenomena are also encountered in the LA-catalyzed Baeyer−Villiger reaction[17a] and 1,3-dipolar cycloaddition between nitrones and alkenes.[17b] In what follows, our major interests will focus on the mechanisms and regio- and stereochemistry of the reactions between aldehyde−

(17) (a) Carlqvist, P.; Eklund, R.; Brinck, T. *J. Org. Chem.* **2001**, *66*, 1193. (b) Tanaka, J.; Kanemasa, S. *Tetrahedron* **2001**, *57*, 899.

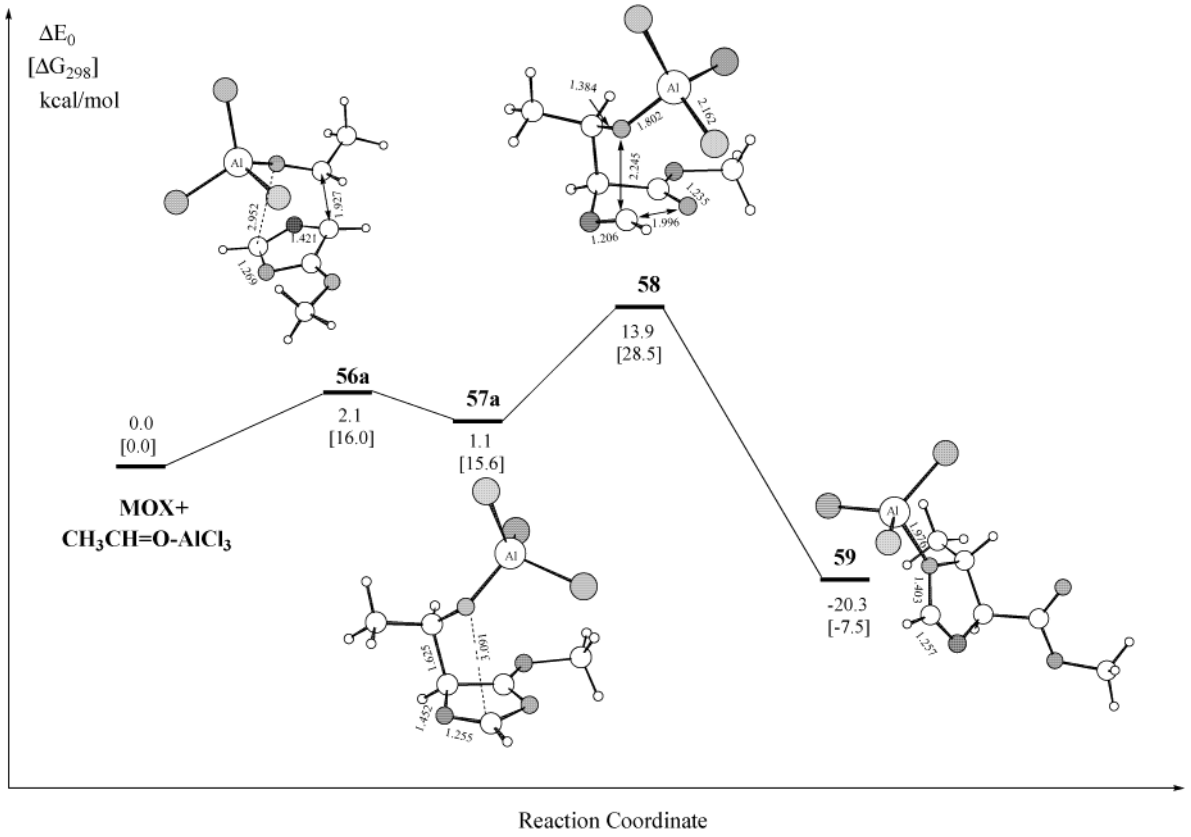

FIGURE 5. The potential energy surface of the C-trans path for reaction IV computed at the B3LYP/6-31G* level. The plain values are energies (kcal/mol) in terms of the gas phase ΔE_0 and ΔG_{298} (in parentheses), respectively.

SCHEME 8

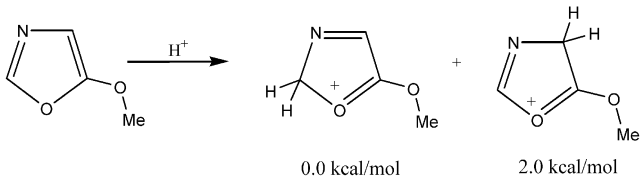

$AlCl_3$ complex and methoxyoxazoles, and therefore, we will not mention this $AlCl_3$-transfer step.

3.2. Three Types of Nuleophilic Addition Transition States. It is well-known that the use of LAs usually can significantly promote rate, regioselectivities, endo/exo selectivities, and diastereofacial selectivities of Diels–Alder reactions.[15,18] Often, when LA is used, the Diels–Alder reaction mechanism may change from concerted to stepwise.[19,20] All efforts (at both HF and DFT levels) to locate a concerted DA reaction transition state between $CH_3CH{=}O{\cdots}AlCl_3$ and MOX were unsuccessful. On the contrary, the nucleophilic attack TSs corresponding to the nucleophilic addition of the C_2 or C_4 of MOX to the carbonyl carbon can be located. Since the final product, 2- or 3-oxazoline, can have cis or trans conformers, we define the path leading to *cis*-/*trans*-3-oxazoline as the A-cis/A-trans path. Similarly, the C-cis/C-trans path in the C manifold can afford *cis*-/*trans*-2-oxazoline.

According to the different orientations between the C=O fragment and 5-alkoxyoxazole, there are three types of NA reaction transition states for the initial step of each reaction path, as shown in Scheme 4. The first type is defined as type **a**, in which the NA TS adopts a Diels–Alder-like conformation. This type of NA reaction is expected to be the favored one, due to the favorable orbital overlap as well as electrostatic attraction between carbonyl-O and the MOX moieties, which possess negative and positive charges in the TS, respectively.[21] When steric and electronic effects, such as the lone pair–lone pair repulsions of O_8 with O_1 and O_6, are taken into account, two more types of NA reactions could become competitive. These two types of NA reactions could adopt either **b** or **c** conformations, where the C=O fragment in the NA TSs is antiperiplanar (**b** type) or gauche (**c** type) to the $C_2{=}N_3$ (manifold A) or the $C_4{=}C_5$ (manifold C) (Scheme 4).

(18) (a) Yates, P.; Eaton, P. *J. Am. Chem. Soc.* **1960**, *82*, 4436. (b) Jorgensen, K. A. *Angew. Chem., Int. Ed.* **2000**, *39*, 3558. For recent reviews of Diels–Alder reactions, see: (c) Corey, E. J. *Angew. Chem., Int. Ed.* **2002**, *41*, 1650. (d) Nicolaou, K. C.; Snyder, S. A.; Montagnon, T.; Vassilikogiannakis, G. *Angew. Chem., Int. Ed.* **2002**, *41*, 1668.

(19) For stepwise LA catalyzed Diels–Alder reactions, see for example: (a) Danishefsky, S. J.; Selnick, H. G.; Zelle, R. E.; Deninno, M. F. *J. Am. Chem. Soc.* **1988**, *110*, 4368. (b) Roberson, M.; Jepsen, A. S.; Jorgensen, K. A. *Tetrahedron* **2001**, *57*, 907.

(20) For concerted LA-catalyzed Diels–Alder reaction, see, for example: (a) Singleton, D. A.; Merrigan, S. R.; Beno, B. R.; Houk, K. N. *Tetrahedron Lett.* **1999**, *40*, 5817. (b) Yamabe, S.; Dai, T.; Minato, T. *J. Am. Chem. Soc.* **1995**, *117*, 10994. (c) Garcia, J. I.; Martinez-Merino, V.; Mayoral, J. A.; Salvatella, L. *J. Am. Chem. Soc.* **1998**, *120*, 2415. (d) Birney, D. M.; Houk, K. N. *J. Am. Chem. Soc.* **1990**, *112*, 4127. (e) McCarrick, M. A.; Wu, Y.-D.; Houk, K. N. *J. Org. Chem.* **1993**, *58*, 3330.

(21) Casiraghi, G.; Rassu, G.; Zanardi, F.; Battistini, L. *Advances in Asymmetric Synthesis*; Hassner, A., Ed.; JAI Press INC: Stamford, Connecticut, 1998; Vol. 3, p 113.

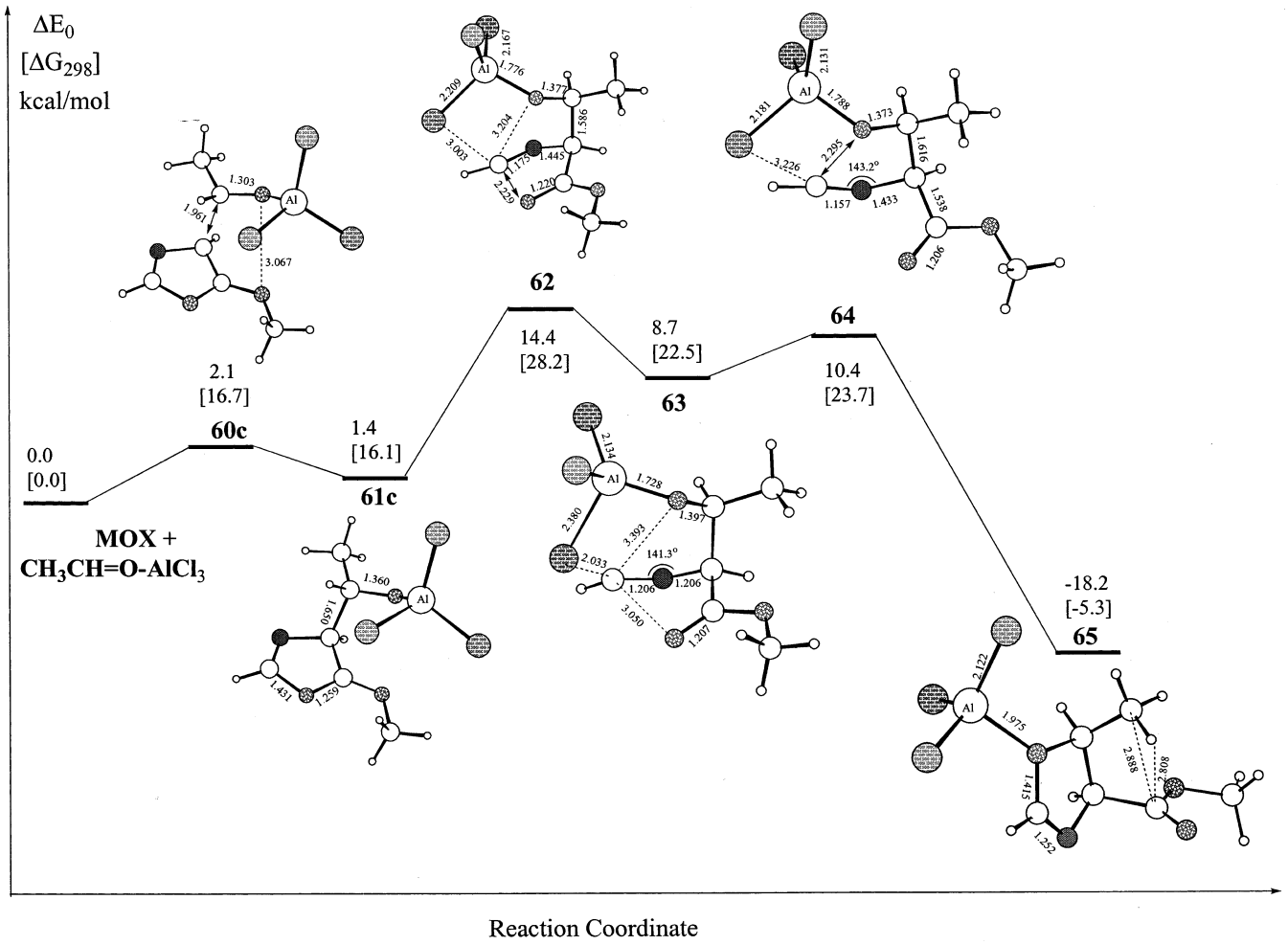

FIGURE 6. The potential energy surface of the C-cis path for reaction IV computed at the B3LYP/6-31G* level. The plain values are energies (kcal/mol) in terms of the gas phase ΔE_0 and ΔG_{298} (in parentheses), respectively.

All the possible NA reactions of acetaldehyde with the C_2 and C_4 of MOX have been searched; their relative energies in each path are summarized in Scheme 4. The energies of the lowest energy NA TS in each path with respect to reactants are summarized in Scheme 5 (their structures will be given below). The Diel-Alder-like NA TSs are preferred for two of the four paths. Even in the A-cis path, the Diels−Alder-like TS **50a** is only slightly less stable than antiperiplanar TS **50b** by 0.4 kcal/mol. The reason that **50b** is preferred over **50a** is due to the lone-pair−lone pair repulsion between the carbonyl oxygen O_8 and the O_1 of MOX (denoted O_8–O_1 repulsion, as shown in Scheme 6) in the latter TS. Due to the loss of favorable attraction of O_8 to the positively charged oxazole moiety, **50b** is less stable than **44a** by 1.1 kcal/mol.

The located Diels−Alder-like NA TS in the C-cis path is **60a**, in which the $AlCl_3$ is in the cis arrangement with the methyl group of aldehyde. This is certainly caused by the O_8–O_1 repulsion, since all efforts to locate a DA-like TS with a trans orientation of $AlCl_3$ to methyl group of the acetaldehyde led to **60a** (Scheme 7). This is more evidence to support the suggestion that the O_8–O_1 repulsion should be avoided in the reaction process. As we will show later, this O−O repulsion is the major factor affecting the stereochemistry of reactions IV and V. Due to the unfavorable cis configuration, **60a** is 1.9 kcal/mol less stable than **60c**, which is free of serious steric and electronic repulsions. The NA TS **56a** is also in the Diels−Alder-like conformation. The gauche **56c** is less stable than **56a** by 2.7 kcal/mol, mainly due to O_8–O_6 repulsion (Scheme 4).

Similarly, the zwitterionic intermediate generated by the NA reaction also has the abovementioned three kinds of conformations, which prefer the Diels−Alder-like conformations when other factors such as solvent effect are not taken into account. The other stationary points involved in reactions IV and V share the same conformational preferences. Therefore, to be concise for later discussions, the structures and energies for all the reactions discussed are those in their most stable conformations.

3.3. Reaction IV (MOX + CH_3CH=O···$AlCl_3$). The potential energy surface of reaction IV is given in Figure 2. The structures and relative energies of the species involved in each path are shown in Figures 3 (A-trans), 4 (A-cis), 5 (C-trans), and 6 (C-cis), respectively. The calculated energies as well as other parameters are given in the Supporting Information. From Figure 2, we can see that the overall activation energies for the A-trans, A-cis, C-trans, and C-cis paths are 3.0, 3.9, 13.9, and 14.4 kcal/mol, respectively, implying that manifold A is fa-

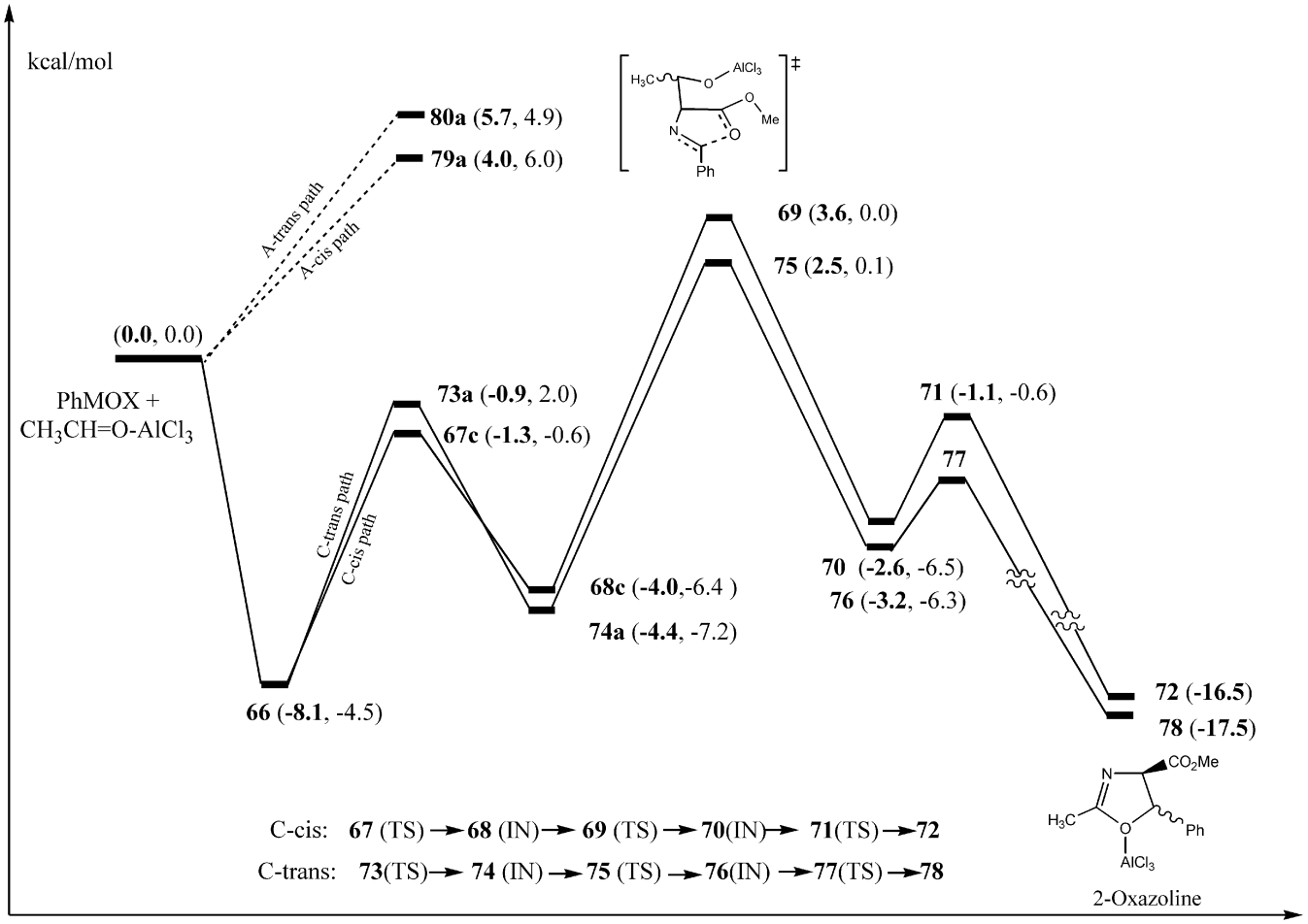

FIGURE 7. The potential energy surface for reaction V computed at the B3LYP/6-31G* level. The bold and plain values in parentheses are energies (kcal/mol) in terms of gas phase ΔE_{ele} and solvent $\Delta E_{ele}(CH_2Cl_2)$, respectively.

SCHEME 9

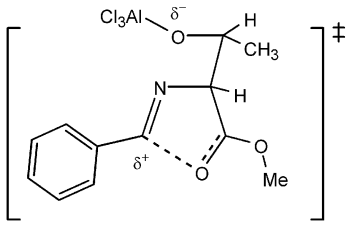

SCHEME 10

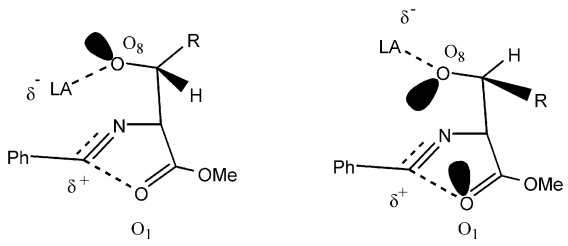

vored, yielding 3-oxazoline, which is dominated by the trans conformer. These results clearly show that both the LA-catalyzed and uncatalyzed reactions intrinsically favor the path to give *trans*-3-oxazoline. The major difference is certainly related to the activation energies of 3.0 and 30.5 kcal/mol for the LA-catalyzed and uncatalyzed reactions, respectively, showing a significant acceleration of the cyclization of aldehyde to MOX by LA catalysts.

(a) Mechanism. Both the A-trans and A-cis paths occur readily with similar mechanism, which starts with NA reaction of the C_2 of MOX to the carbonyl carbon of acetaldehyde to form zwitterionic intermediates (ZW-IN) **45** and **51**, respectively.[22] Not only does this NA reaction have lower activation energy, but it is also slightly exothermic (about 4.5 and 2.7 kcal/mol for A-trans and A-cis paths, respectively). As we pointed out in the previous paper, the bottleneck for the uncatalyzed reaction of aldehyde with MOX is the RORC step, which needs about 25.5 kcal/mol because the anionic aldehyde oxygen cannot be efficiently stabilized.[1] Here we can see that owing to the complexation of acetaldehyde oxygen by $AlCl_3$, the activation energies of the RO steps are only 7.5 and 6.4 kcal/mol for the A-trans and A-cis paths, respectively.

Despite the slight endothermicities of the RO steps in manifold A, the last RC steps to furnish 3-oxazoline are very facile, with activation energies less than 2 kcal/mol.

(22) A complex between MOX and $CH_3CHO-AlCl_3$ is expected to be formed before the NA reaction. In the gas phase, the location of such a precursor complex led to the bond formation between N_3 and the carbonyl carbon of aldehyde. This artificial phenomenon can be avoided in solvent due to the dampened interaction between the two reactants. As shown later in reaction VI, such a precursor complex **66** in reaction VI can be located in the gas phase.

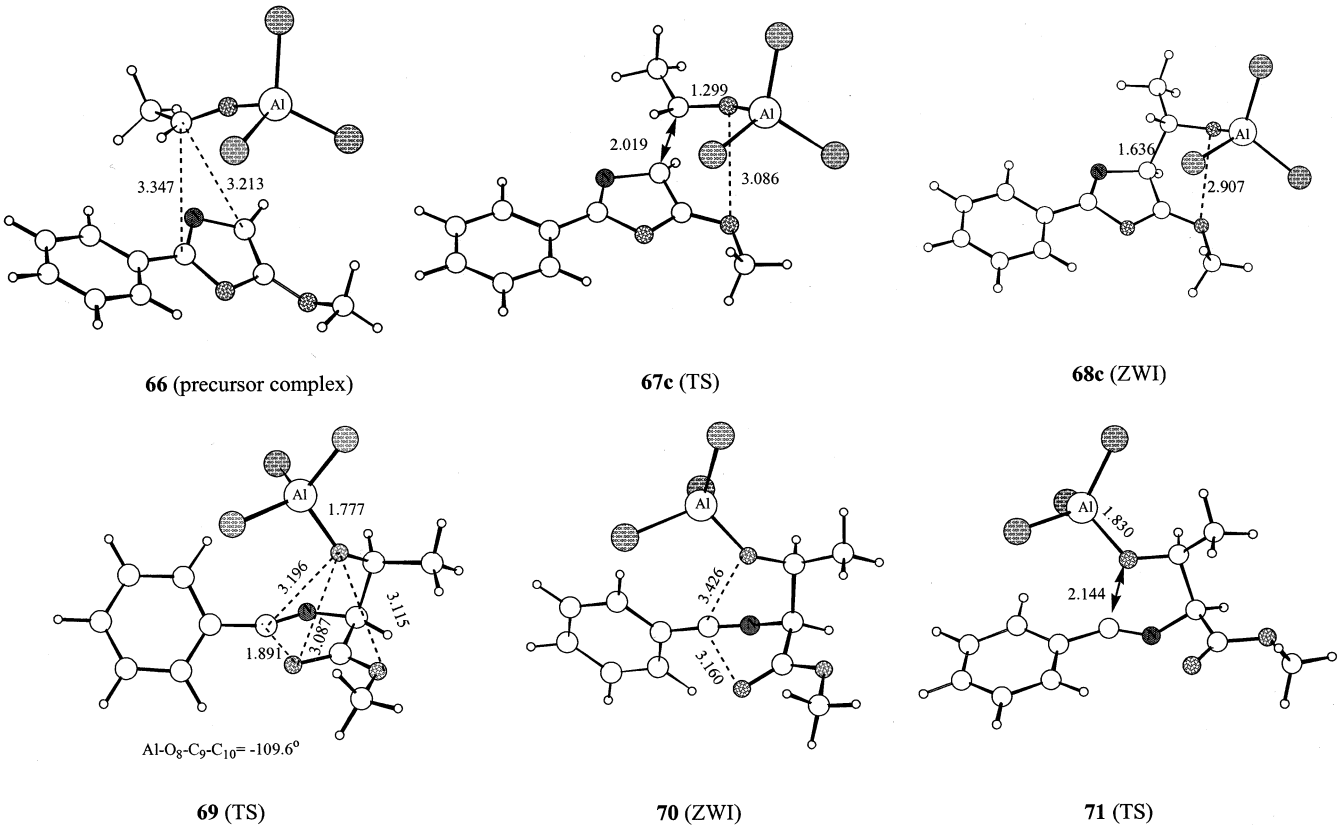

66 (precursor complex) **67c** (TS) **68c** (ZWI)

69 (TS) **70** (ZWI) **71** (TS)

FIGURE 8. The geometries for the key species of reaction V in the C-cis path computed at the B3LYP/6-31G* level. Distances are in angstroms.

The overall reaction is very exothermic. The *trans*-3-oxazoline−$AlCl_3$ complex is more stable than the *cis*-3-oxazoline−$AlCl_3$ complex, in contrast to the free 3-oxazolines, where the cis conformer is more stable than the trans conformer.[1]

The C-cis path leading to *cis*-2-oxazoline−$AlCl_3$ takes place in a similar manner as the A-trans and A-cis paths (Figure 6). By contrast, the C-trans path occurs in a two-step process, where the NA adduct **57a** is transformed to *trans*-2-oxazoline−$AlCl_3$ via a concerted RORC step. Compared to the uncatalyzed reaction, the activation energies of both the NA and RORC steps are reduced. The overall activation energies of the C-trans and C-cis paths are still as high as 14 kcal/mol. Therefore, the favored reaction mechanism is manifold A instead of manifold C.

(b) Origin of the Preference for Manifold A. Three factors can be identified to explain why manifold A is favored over manifold C. One is due to the endothermicity of the NA reaction in manifold C, leading the NA adducts in this manifold to lie higher than their counterparts in manifold A by about 4 kcal/mol. This difference is attributed to the ability of the MOX moiety to stabilize the partial positive charge in it, which is caused by the charge transfer of MOX to $CH_3CH{=}O{-}AlCl_3$. This difference can be understood through comparing the protonation reaction of MOX, which favors the generation of a cation at the C_2 rather than at the C_4 position of MOX by about 2.0 kcal/mol (Scheme 8).

The second factor is apparently due to the high activation energies of the RO and RORC steps in the C manifold compared to those of the RO steps in manifold A (the average activation barriers are 7.0 and 13.0 for manifolds A and C, respectively; Figure 2). We can see that in the RO or RORC transition states, a carbocation at the C_2 atom has been created due to the cleavage of the C_2–O_1 bond. The large difference in the rate-determining transition states for the two manifolds lies in the fact that C_2 is sp^3 for manifold A and sp^2 for manifold C. The cleavage of the C_2–O_1 bond is much more difficult for manifold C than for manifold A (recall that the sp^3 carbocation is much more stable than the sp^2 carbocation).

The third factor for the regioselectivity is the conjugation effect. The positive charge in the oxazole fragment of the RORC TSs of manifold A can be stabilized by delocalizing the charge, while in RO or RORC TSs of manifold C, the conjugation is lost, since the C_3 atom is tetrahedral (see Figure 2).

(c) The Origin of the Trans Diastereoselectivity. For the favored manifold A, the transition states of the NA and RO steps have similar energies both in the gas phase and solution (Figure 2; the solvent effect will be discussed in the next section). Therefore, which step is rate-determining is likely affected by many factors, such as solvent and presence of various substituents. However, calculations indicate a preference for trans diastereoselectivity, no matter which step is rate-determining. This diastereoselectivity is most likely due to the electrostatic repulsion between O_8 and O_1 in the transition states of the A-cis path (see Scheme 6 and their transition structures in Figure 4).

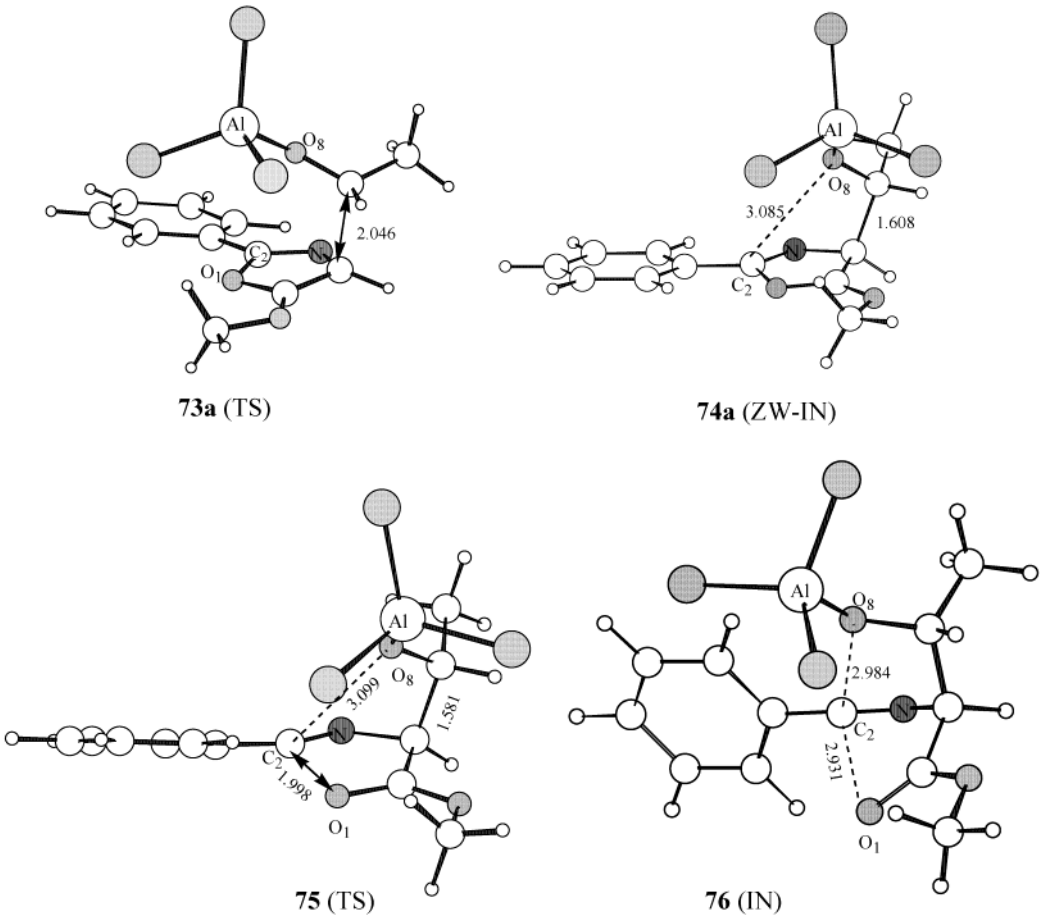

FIGURE 9. The geometries for the key species of reaction V in the C-trans path computed at the B3LYP/6-31G* level. Distances are in angstroms.

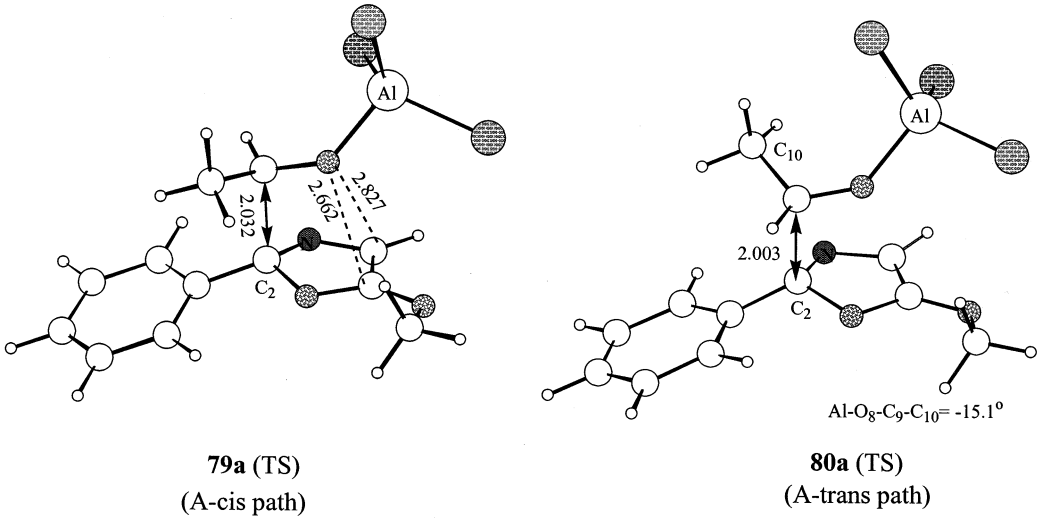

FIGURE 10. The geometries of the two NA TSs in the A-cis and A-trans paths of reaction V computed at the B3LYP/6-31G* level. Distances are in angstroms.

(d) Solvent Effects. It is expected that solvent can influence the stereochemistry significantly, especially for those reactions involving the generation of highly polar transition states and intermediates. Manifold A has such a large fluctuation of the dipole moments during the reaction course (see their dipole moments in the Table S1). For example, the dipole moments for **44**, **45**, and **46** are 8.60, 11.83, and 12.50 D, respectively. We investigated this reaction in CH_2Cl_2 by using the PCM model. The calculated relative energies $\Delta E_0(CH_2Cl_2)$ are given in Figure 2. Here we can see that the regiochemistry favoring manifold A yielding 3-oxazoline is not affected by solvent. The primary influence exerted by solvent is the switching of the rate-determining step from being the

RO step in the gas phase to the NA step in solvent. This change is understandable, since it is expected that the polar solvent can stabilize RO TSs more efficiently than the NA TSs, due to the larger dipole moment of the former than the latter. However, the overall activation energies for both the favored A-trans and A-cis paths are almost the same [A-trans, 3.0 (gas phase) and 3.1 kcal/mol (CH_2Cl_2); A-cis, 3.9 (gas phase) and 3.6 kcal/mol (CH_2Cl_2)].

In summary, theoretical calculations predict that the LA-catalyzed reaction of aldehydes with 5-alkoxyloxazole intrinsically favors the generation of 3-oxazoline with the trans conformer as the major product. The regiochemistry is not affected by solvent.

3.4. Reaction V ($CH_3CH{=}O{\cdots}AlCl_3$ + PhMOX). The potential energy surfaces of reaction V, both in the gas phase and in CH_2Cl_2, are shown in Figure 7. The structures of all stationary points are given in Figures 8 (C-trans), 9 (C-cis), and 10 (A-trans and A-cis). Figure 7 clearly shows that manifold C is favored, generating 2-oxazoline, due to the fact that the overall activation energies in both the gas phase and solvent are lower than the NA TSs of the A-trans and A-cis paths. The mechanism for the transformation of the C-trans and C-cis paths is similar to those of reaction IV and will not be discussed further.[22,23]

(a) Origin of the Preference of Manifold C Leading to the Generation of 2-Oxazoline. The potential energy surfaces of reaction V clearly show that two factors are responsible for the preference for manifold C. One reason for this is associated with the NA reaction. The NA TSs in manifold A are disfavored due to the disruption of the conjugation between oxazole and the phenyl ring when the C_2 of PhMOX adds to the aldehyde carbonyl carbon. The NA TSs are about 6 kcal/mol less stable than their counterparts in manifold C in the gas phase (Figure 7).

On the other hand, the activation energies of the RO steps are now reduced to 6.9 (C-trans) and 7.4 kcal/mol (C-cis), about 6 kcal/mol lower than those in reaction IV without the Ph group at the C_2 position. The Ph group significantly reduces the activation energy by stabilizing the C_2 carbocation in the RO transition state via conjugation, as shown in Scheme 9.

(b) Stereochemistry. In the gas phase, the C-trans path is favored over the C-cis path by 1.1 kcal/mol in terms of ΔE_{ele}, ΔE_0, and ΔG_{298}. Comparison of the rate-determining TSs **69** and **75** clearly indicates that the O−O repulsions of carbonyl oxygen O_8 to O_1 and O_6 are responsible for the higher energy of C-cis RO TS **69** compared to C-trans RO TS **75**, which benefits from the attraction between carbonyl oxygen and the C_2 carbocation instead (see Scheme 10 and Figures 8 and 9). In CH_2Cl_2, the manifold C is still favored. The product is dominated by the *cis*-2-oxazoline, since the rate-determining step in the C-cis path is RO TS **69** which is about 2.0 kcal/mol lower than the rate-determining NA TS **73a** of the C-trans path (Figure 7). The different stereochemistry in the gas phase and solvent suggests that the solvent used affects the stereochemical outcome. It is also expected that different LA catalysts with different sizes and acidities will also influence the regiochemistry, as unveiled by Suga and Ibata's experiments.[3,24] The aggregation of the catalyst (for example, $TiCl_4$) would also affect the stereochemical results.[15] It is difficult to include all these effects in the theoretical study of the stereochemistry. Our results here can identify that the electronic effect, the O−O repulsion, in the transition states is one major factor influencing stereochemistry. When steric effects are introduced by bulky catalysts, the stereochemical outcomes can be altered to some extent. This is the case achieved by Evans' Salen−aluminum complexes,[4] and our theoretical study for this system will be reported in due course.

4. Conclusions

Density functional theory calculations on the Lewis acid-catalyzed reactions between 5-methoxyoxazoles and aldehydes reveal that these reactions start from the complexation of LA to 5-methoxyoxazoles, then an $AlCl_3$-transfer process transfers $AlCl_3$ from 5-methoxyoxazole−$AlCl_3$ complexes to aldehydes (Figure 1). The resulting 5-methoxyoxazoles and aldehyde−$AlCl_3$ complexes (denoted as reactions IV and V) efficiently take part in the followed reactions via a stepwise mechanism (Scheme 3). Reactions IV and V start with nucleophilic addition (NA) of either C_2 (manifold A) or C_4 (manifold C) of 5-alkoxyoxazole to an aldehyde, leading to a zwitterionic intermediate. This is followed by either a concerted ring-opening−ring-closing step or stepwise ring-opening and ring-closing steps. Compared to the uncatalyzed reaction, the presence of the Lewis acid reduces the activation energy significantly, because it stabilizes zwitterionic transition states and intermediates.

Reaction IV strongly prefers manifold A, leading to 3-alkoxycarbonyl-3-oxazoline. This is because the cation generated at the C_2 in the RO transition state is more stable (sp^3) for manifold A than for manifold C (sp^2). Conjugation also favors manifold A. For reaction V, the presence of a phenyl group at C_2 can stabilize the sp^2 carbocation in manifold C. On the other hand, manifold A loses conjugation between the phenyl group and the $C_2{=}N_3$ bond when nucleophilic addition happens. Therefore, manifold C becomes favored for reaction V, resulting in the formation of 4-alkoxycarbonyl-2-oxiazoline. The trans stereoselectivity for the catalyzed reaction can be understood in terms of O_8–O_1 repulsion in the NA or RO transition states in the gas phase (see Scheme 10). Solvent, substituent, and catalysts are expected to affect this trans stereoselectivity.

(23) All attempts to locate the ring-closing TS or a concerted RORC corresponding to O_1–C_2 bond breaking and O_8–C_2 bond forming in the C-trans path in the reaction V were not successful. We think that RC transition state **77** should exist with very low activation barrier given the fact that all the RC steps located for reactions IV and V have very low activation barriers.

(24) Substituent effects will also affect the cis and trans stereochemistry. For example, if the aldehyde−$AlCl_3$ complex used is PhCH=O−$AlCl_3$ (most of the aldehydes used are aromatic aldehydes in Suga's experiment), we found that the trans selectivity is reproduced (see Figure S2 in the Supporting Information). Again, the O_8–O_1 repulsion is invoked to explain the lower stability of the C-cis RO TS **82** with respect to the C-trans RO TS **84**. In **82**, the Al−O_8–C(Ph) is near perpendicular to the Ph plane in order to reduce the O_8–O_1 repulsion if the Ph and $AlCl_3$ are in the trans configuration. Despite this conformation change, **82** still suffers from strong O_8–O_1 repulsion, due to their close contact (the distance of O_8–O_1 is 2.914 Å). By contrast, C-trans RO TS **84** benefits from the attraction of the lone pair of O_8 to the cationic C_2. Here we see again that the rate-determining step for the manifold C is the RO step.

This study establishes a solid foundation for the study of the mechanism and stereochemistry of the reaction of 5-alkoxyoxazoles with aldehydes catalyzed by bulky and chiral Lewis acids, such as (R)-BINOL−AlMe and Salen−aluminum complexes, and for the design of new effective catalysts.[25]

Acknowledgment. We are grateful to the Research Grants Council of Hong Kong for financial support of the work. Y.-D.W. also thanks the Croucher Foundation for a Croucher Senior Research Fellowship award. Z.-X.Y. is indebted to Prof. K. N. Houk and Drs. A. G. Leach and B. N. Hietbrink for fruitful discussions. We are especially indebted to the referees who gave particularly constructive suggestions for the improvement of the manuscript.

(25) Semiempirical calculations by the PM3 method gave opposite stereochemistry to that of DFT calculations, suggesting that high-level ab initio calculations are needed to investigate the mechanism and sterochemistry of the reaction catalyzed by Evans' catalysts.[4]

Supporting Information Available: Tables S1 and S2 containing the calculated energies, dipole moments, and other thermodynamic parameters for the stationary points discussed in reactions IV and V; the Cartesian coordinates of all species are also included; and the potential energy surfaces for the $AlCl_3$-transfer process and the reaction of PhCH═O and PhMOX are given in Figures S1 and S2. This material is available free of charge via the Internet at http://pubs.acs.org.

JO0263317